Cell

DICER1 Loss and *Alu* RNA Induce Age-Related Macular Degeneration via the NLRP3 Inflammasome and MyD88

Valeria Tarallo,[1,16] Yoshio Hirano,[1,16] Bradley D. Gelfand,[1,16] Sami Dridi,[1] Nagaraj Kerur,[1] Younghee Kim,[1] Won Gil Cho,[1,3] Hiroki Kaneko,[1] Benjamin J. Fowler,[1,2] Sasha Bogdanovich,[1] Romulo J.C. Albuquerque,[1] William W. Hauswirth,[4] Vince A. Chiodo,[4] Jennifer F. Kugel,[5] James A. Goodrich,[5] Steven L. Ponicsan,[5] Gautam Chaudhuri,[6] Michael P. Murphy,[7] Joshua L. Dunaief,[8] Balamurali K. Ambati,[9,10] Yuichiro Ogura,[11] Jae Wook Yoo,[12] Dong-ki Lee,[12] Patrick Provost,[13] David R. Hinton,[14] Gabriel Núñez,[15] Judit Z. Baffi,[1] Mark E. Kleinman,[1] and Jayakrishna Ambati[1,2,*]

[1]Department of Ophthalmology & Visual Sciences
[2]Department of Physiology
University of Kentucky, Lexington, KY 40506, USA
[3]Department of Anatomy, Yonsei University Wonju College of Medicine, Wonju City 220-701, Korea
[4]Department of Ophthalmology, University of Florida, Gainesville, FL 32610, USA
[5]Department of Chemistry and Biochemistry, University of Colorado at Boulder, Boulder, CO 80309, USA
[6]Department of Microbiology and Immunology, Meharry Medical College, Nashville, TN 37208, USA
[7]MRC Mitochondrial Biology Unit, MRC/Wellcome Trust Building, Hills Road, Cambridge CB2 0XY, UK
[8]F.M. Kirby Center for Molecular Ophthalmology, Scheie Eye Institute, University of Pennsylvania, Philadelphia, PA 19104, USA
[9]Department of Ophthalmology and Visual Sciences, Moran Eye Center, University of Utah School of Medicine, Salt Lake City, UT 84132, USA
[10]Department of Ophthalmology, Veterans Affairs Salt Lake City Healthcare System, Salt Lake City, UT 84148, USA
[11]Department of Ophthalmology and Visual Science, Nagoya City University Graduate School of Medical Sciences, Nagoya 467-8601, Japan
[12]Global Research Laboratory for RNAi Medicine & BK21 School of Chemical Materials Science and Department of Chemistry, Sungkyunkwan University, Suwon 440-746, Korea
[13]CHUL Research Center/CHUQ and Faculty of Medicine, Université Laval, Quebec QC G1K 7P4, Canada
[14]The Arnold and Mabel Beckman Macular Research Center at the Doheny Eye Institute, University of Southern California, Los Angeles, CA 90033, USA
[15]Department of Pathology and Comprehensive Cancer Center, University of Michigan Medical School, Ann Arbor, MI 48109, USA
[16]These authors contributed equally to this work
*Correspondence: jamba2@email.uky.edu
DOI 10.1016/j.cell.2012.03.036

SUMMARY

Alu RNA accumulation due to DICER1 deficiency in the retinal pigmented epithelium (RPE) is implicated in geographic atrophy (GA), an advanced form of age-related macular degeneration that causes blindness in millions of individuals. The mechanism of *Alu* RNA-induced cytotoxicity is unknown. Here we show that DICER1 deficit or *Alu* RNA exposure activates the NLRP3 inflammasome and triggers TLR-independent MyD88 signaling via IL18 in the RPE. Genetic or pharmacological inhibition of inflammasome components (NLRP3, Pycard, Caspase-1), MyD88, or IL18 prevents RPE degeneration induced by DICER1 loss or *Alu* RNA exposure. These findings, coupled with our observation that human GA RPE contains elevated amounts of NLRP3, PYCARD, and IL18 and evidence of increased Caspase-1 and MyD88 activation, provide a rationale for targeting this pathway in GA. Our findings also reveal a function of the inflammasome outside the immune system and an immunomodulatory action of mobile elements.

INTRODUCTION

Age-related macular degeneration (AMD) affects the vision of millions of individuals (Smith et al., 2001). AMD is characterized by degeneration of the retinal pigmented epithelium (RPE), which is situated between the retinal photoreceptors and the choroidal capillaries (Ambati et al., 2003). RPE dysfunction disrupts both photoreceptors and choroidal vasculature (Blaauwgeers et al., 1999; Lopez et al., 1996; McLeod et al., 2009; Vogt et al., 2011). These tissue disruptions lead to atrophic or neovascular disease phenotypes. Although there are therapies for neovascular AMD, there is no effective treatment for the more common atrophic form. Geographic atrophy (GA), the advanced stage of atrophic AMD, is characterized by degeneration of the RPE and is the leading cause of untreatable vision loss.

Recently we showed that a dramatic and specific reduction of the RNase DICER1 leads to accumulation of *Alu* RNA transcripts in the RPE of human eyes with GA (Kaneko et al., 2011). These repetitive element transcripts, which are noncoding RNAs

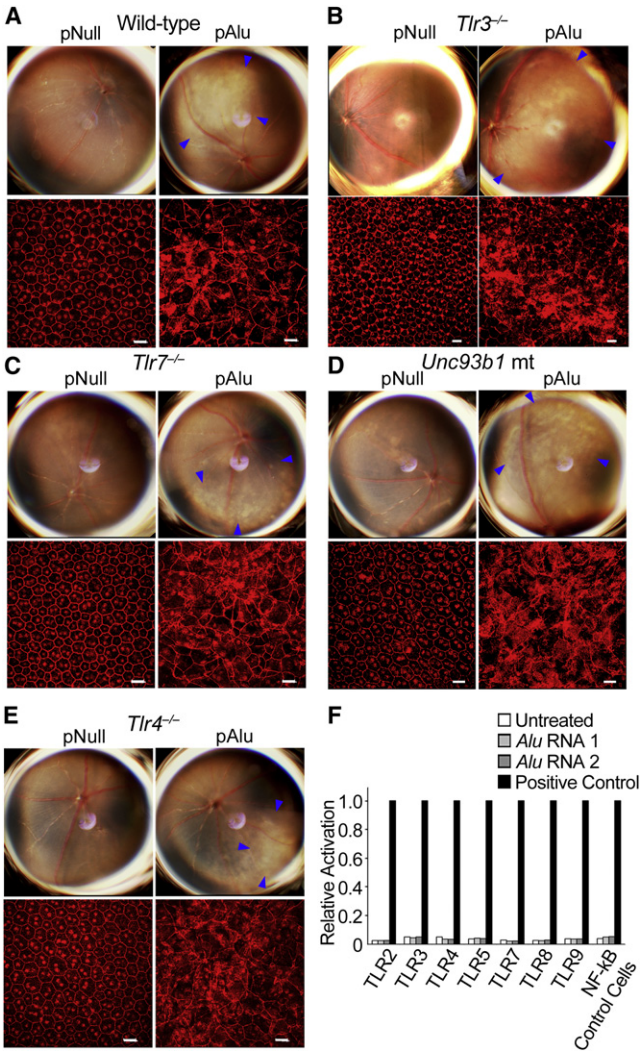

Figure 1. *Alu* RNA Does Not Activate or Function via TLRs

(A–E) pAlu, but not pNull, induces RPE degeneration in WT (A), *Tlr3*$^{-/-}$ mice (B), *Tlr7*$^{-/-}$ mice (C), *Unc93b1 mt* mice, which are functionally deficient in TLRs 3, 7, 9 (D), and *Tlr4*$^{-/-}$ mice (E). Representative images shown. n = 8–12. Fundus photographs, top row; flat mounts stained for zonula occludens-1 (ZO-1; red), bottom row. Degeneration outlined by blue arrowheads. Scale bars, 20 μm.

(F) Stimulation of HEK293 cell lines expressing various TLRs with either of two different *Alu* RNA sequences does not elicit NF-κB activation. Positive (+) controls using TLR-specific ligands activated NF-κB. n = 3.

See also Figure S1.

expressed by the highly abundant *Alu* retrotransposon (Batzer and Deininger, 2002), induce human RPE cell death and RPE degeneration in mice. DICER1 deficit in GA RPE was not a generic cell-death response because DICER1 expression was not dysregulated in other retinal diseases. Likewise, *Alu* RNA accumulation did not represent generalized retrotransposon activation due to a stress response in dying cells because other retrotransposons were not elevated in GA RPE.

DICER1 is central to mature microRNA (miRNA) biogenesis (Bernstein et al., 2001). Yet following DICER1 deficit, the accumulation of *Alu* RNA and not the lack of mature miRNAs was the critical determinant of RPE cell viability (Kaneko et al., 2011). Moreover, 7SL RNA, transfer RNA, and primary miRNAs do not induce RPE degeneration (Kaneko et al., 2011), ruling out a nonspecific toxicity of excess, highly structured RNA. Still, the precise mechanisms of *Alu* RNA cytotoxicity are unknown.

Although the retina is exceptional for its immune privilege (Streilein, 2003), insults mediated by innate immune sensors can result in profound inflammation. The three major classes of innate immune receptors include the toll-like receptors (TLRs), RIG-I-like helicases, and NLR proteins (Akira et al., 2006). Numerous innate immune receptors are expressed in the RPE (Kumar et al., 2004), and several exogenous substances can induce retinal inflammation (Allensworth et al., 2011; Kleinman et al., 2012). However, it is not known whether this surveillance machinery recognizes or responds to host endogenous RNAs. We explored the concept that innate immune machinery, whose canonical function is the detection of pathogen-associated molecular patterns and other moieties from foreign organisms, might also recognize *Alu* RNA.

Indeed, we show that *Alu* transcripts can hijack innate immunity machinery to induce RPE cell death. Surprisingly, our data show that DICER1 deficit or *Alu* RNA activates the NLRP3 inflammasome in a MyD88-dependent but TLR-independent manner. NLRP3 inflammasome activation in vivo has been largely restricted to immune cells, although our data open up the possibility that NLRP3 activity may be more widespread, as reflected by examples in cell culture studies of keratinocytes (Feldmeyer et al., 2007; Keller et al., 2008). Our data also broaden the scope of DICER1 function beyond miRNA biogenesis and identify DICER1 as a guardian against aberrant accumulation of toxic retrotransposon elements that comprise roughly 50% of the human genome (Lander et al., 2001). In sum, our findings present a novel self-recognition immune response, whereby endogenous noncoding RNA-induced NLRP3 inflammasome activation results from DICER1 deficiency in a nonimmune cell.

RESULTS

Alu RNA Does Not Activate a Variety of TLRs or RNA Sensors

Alu RNA has single-stranded (ss) RNA and double-stranded (ds) RNA motifs (Sinnett et al., 1991). Thus we tested whether *Alu* RNA induced RPE degeneration in mice deficient in TLR3, a dsRNA sensor (Alexopoulou et al., 2001), or TLR7, a ssRNA sensor (Diebold et al., 2004; Heil et al., 2004). Subretinal delivery of a plasmid coding for *Alu* RNA (pAlu) induced RPE degeneration in *Tlr3*$^{-/-}$ and *Tlr7*$^{-/-}$ mice just as in wild-type (WT) mice (Figures 1A–1C). We previously showed that ≥21-nucleotide fully complementary small interfering RNAs (siRNAs) activate TLR3 on RPE cells (Kleinman et al., 2012). Lack of TLR3 activation by *Alu* RNA is likely due to its complex structure containing multiple hairpins and bulges that might preclude TLR3 binding. Neither 7SL RNA, the evolutionary precursor of *Alu* RNA, nor p7SL induced RPE degeneration in WT mice (Figures S1A and S1B available online), suggesting that *Alu* RNA cytotoxicity might be due to as yet unclear structural features. pAlu induced RPE degeneration in *Unc93b1* mice (Figure 1D), which lack TLR3,

TLR7, and TLR9 signaling (Tabeta et al., 2006), indicating that these nucleic acid sensors are not activated by *Alu* RNA redundantly. pAlu induced RPE degeneration in *Tlr4*$^{-/-}$ mice (Figure 1E), and the TLR4 antagonist *Rhodobacter sphaeroides* LPS (Qureshi et al., 1991) did not inhibit pAlu-induced RPE degeneration in WT mice (Figure S1C). Thus the observed RPE cell death is not due to lipopolysaccharide contamination. Further, two different in vitro transcribed *Alu* RNAs (Kaneko et al., 2011) did not activate multiple TLRs (Figure 1F).

Next we tested whether other dsRNA sensors such as MDA5 (Kato et al., 2006) or PKR (encoded by *Prkr*; Yang et al., 1995) might mediate *Alu* RNA toxicity. However, pAlu induced RPE degeneration in *Mda5*$^{-/-}$ and *Prkr*$^{-/-}$ mice (Figures S1D and S1E). We tested whether the 5′-triphosphate on in vitro transcribed *Alu* RNA, which could activate RIG-I or IFIT-1 that sense this moiety (Hornung et al., 2006; Pichlmair et al., 2011), was responsible for RPE degeneration. Dephosphorylated *Alu* RNA induced RPE degeneration in WT mice just as well as *Alu* RNA not subjected to dephosphorylation (Figure S1F), indicating that this chemical group is not responsible for the observed cell death. Indeed a 5′-triphosphate ssRNA that activates RIG-I does not induce RPE degeneration in mice (Kleinman et al., 2012). Further, pAlu induced RPE degeneration in mice deficient in mitochondrial antiviral signaling (MAVS) (Figure S1G), through which RIG-I and MDA-5 signal (Kumar et al., 2006; Sun et al., 2006). Collectively these data pointed to an unforeseen mechanism of *Alu* RNA-induced RPE degeneration not mediated by a wide range of canonical RNA sensors.

Alu RNA Cytotoxicity Is Mediated via MyD88 and IL18

We then tested the involvement of TRIF (encoded by *Ticam1*), an adaptor for TLR3 and TLR4 (Hoebe et al., 2003; Yamamoto et al., 2003), and MyD88, an adaptor for all TLRs except TLR3 (Akira et al., 2006; Alexopoulou et al., 2001; Suzuki et al., 2003). *Alu* RNA induced RPE degeneration in *Ticam1*$^{-/-}$ mice (Figure S2A), consistent with findings in *Tlr3*$^{-/-}$ and *Tlr4*$^{-/-}$ mice. Unexpectedly, neither *Alu* RNA nor two different pAlu plasmids induced RPE degeneration in *Myd88*$^{-/-}$ mice (Figures 2A, S2B, and S2C). Intravitreous delivery of a peptide inhibitor of MyD88 homodimerization (Loiarro et al., 2005) prevented RPE degeneration induced by *Alu* RNA in WT mice, whereas a control peptide did not do so (Figure 2B). A MyD88-targeting siRNA, which was shorter than 21 nucleotides in length to prevent TLR3 activation and conjugated to cholesterol to enable cell permeation (Kleinman et al., 2008), but not a control siRNA inhibited RPE degeneration induced by pAlu in WT mice (Figures 2C–2E). *Myd88*$^{+/-}$ heterozygous mice were protected against *Alu* RNA-induced RPE degeneration (Figures 2F and S2D), corroborating the siRNA studies that partial knockdown of MyD88 is therapeutically sufficient.

MyD88-mediated signal transduction induced by interleukins leads to recruitment and phosphorylation of IRAK1 and IRAK4 (Cao et al., 1996; Kanakaraj et al., 1999; Suzuki et al., 2002, 2003). *Alu* RNA increased IRAK1/4 phosphorylation in human RPE cells (Figure 2G), supporting the concept that *Alu* RNA triggers MyD88 signaling. The MyD88 inhibitory peptide reduced *Alu* RNA-induced IRAK1/4 phosphorylation in human RPE cells (Figure S2E), confirming its mode of action.

Next we assessed whether MyD88 activation mediates *Alu* RNA-induced cell death in human and mouse RPE cell culture systems. Consonant with the in vivo data, pAlu reduced cell viability in WT but not *Myd88*$^{-/-}$ mouse RPE cells (Figure 2H). The MyD88-inhibitory peptide, but not a control peptide, inhibited cell death in human RPE cells transfected with pAlu (Figure 2I). Together, these data indicate that MyD88 is a critical mediator of *Alu* RNA-induced RPE degeneration.

MyD88 is generally considered an adaptor of immune cells (O'Neill and Bowie, 2007). However, *Alu* RNA induced cell death via MyD88 in RPE monoculture. Thus, we tested whether *Alu* RNA-induced RPE degeneration in mice was also dependent solely on MyD88 activation in RPE cells. Conditional ablation of MyD88 in the RPE by subretinal injection of AAV1-*BEST1*-Cre in *Myd88*$^{f/f}$ mice protected against *Alu* RNA-induced RPE degeneration (Figures 2J and S2F). Consistent with this finding, *Alu* RNA induced RPE degeneration in WT mice receiving *Myd88*$^{-/-}$ bone marrow but did not do so in *Myd88*$^{-/-}$ mice receiving WT bone marrow (Figure S2G). Collectively, these results indicate that MyD88 expression in the RPE, and not in circulating immune cells, is critical for *Alu* RNA-induced RPE degeneration. These findings comport with histopathological studies of human GA tissue that show no infiltration of immune cells in the area of pathology (C.A. Curcio, H.E. Grossniklaus, G.S. Hageman, and L.V. Johnson, personal communication).

Although MyD88 is critical in TLR signaling (O'Neill and Bowie, 2007), MyD88 activation by *Alu* RNA was independent of TLR activation. Thus, we examined other mechanisms of MyD88 involvement. MyD88 can regulate IFN-γ signaling by interacting with IFN-γ receptor 1 (encoded by *Ifngr1*) (Sun and Ding, 2006). However, pAlu induced RPE degeneration in both *Ifng*$^{-/-}$ and *Ifngr1*$^{-/-}$ mice (Figures S2H and S2I). MyD88 is also essential in interleukin-1 signaling (Muzio et al., 1997). Thus, we tested whether IL1β and the related cytokine IL18, both of which activate MyD88 (Adachi et al., 1998), mediated *Alu* RNA cytotoxicity. Interestingly, whereas *Alu* RNA overexpression in human RPE cells increased IL18 secretion, IL1β secretion was barely detectable (Figure 2K).

Recombinant IL18 induced RPE degeneration in WT but not *Myd88*$^{-/-}$ mice (Figure 2L). IL18 neutralization protected against pAlu-induced RPE degeneration in WT mice, but IL1β did not (Figures 2M and 2N). Also, pAlu induced RPE degeneration in *Il1r1*$^{-/-}$ mice but not *Il18r1*$^{-/-}$ mice (Figures S2J and S2K). These data indicate that IL18 is an effector of *Alu* RNA-induced cytotoxicity.

Alu RNA Activates the NLRP3 Inflammasome

We explored whether Caspase-1 (encoded by *Casp1*), a protease that induces maturation of interleukins into biologically active forms (Ghayur et al., 1997; Gu et al., 1997; Thornberry et al., 1992), was involved in *Alu* RNA-induced RPE degeneration. *Alu* RNA treatment of human RPE cells led to Caspase-1 activation as measured by western blotting and by a fluorescent reporter of substrate cleavage (Figures 3A and S3A). Indeed, *Alu* RNA induced Caspase-1 activation in other cell types such as HeLa and THP-1 monocytic cells (Figure S3B), suggesting that *Alu* RNA cytotoxicity has potentially broad implications in many systems. Intravitreous delivery of the Caspase-1-inhibitory

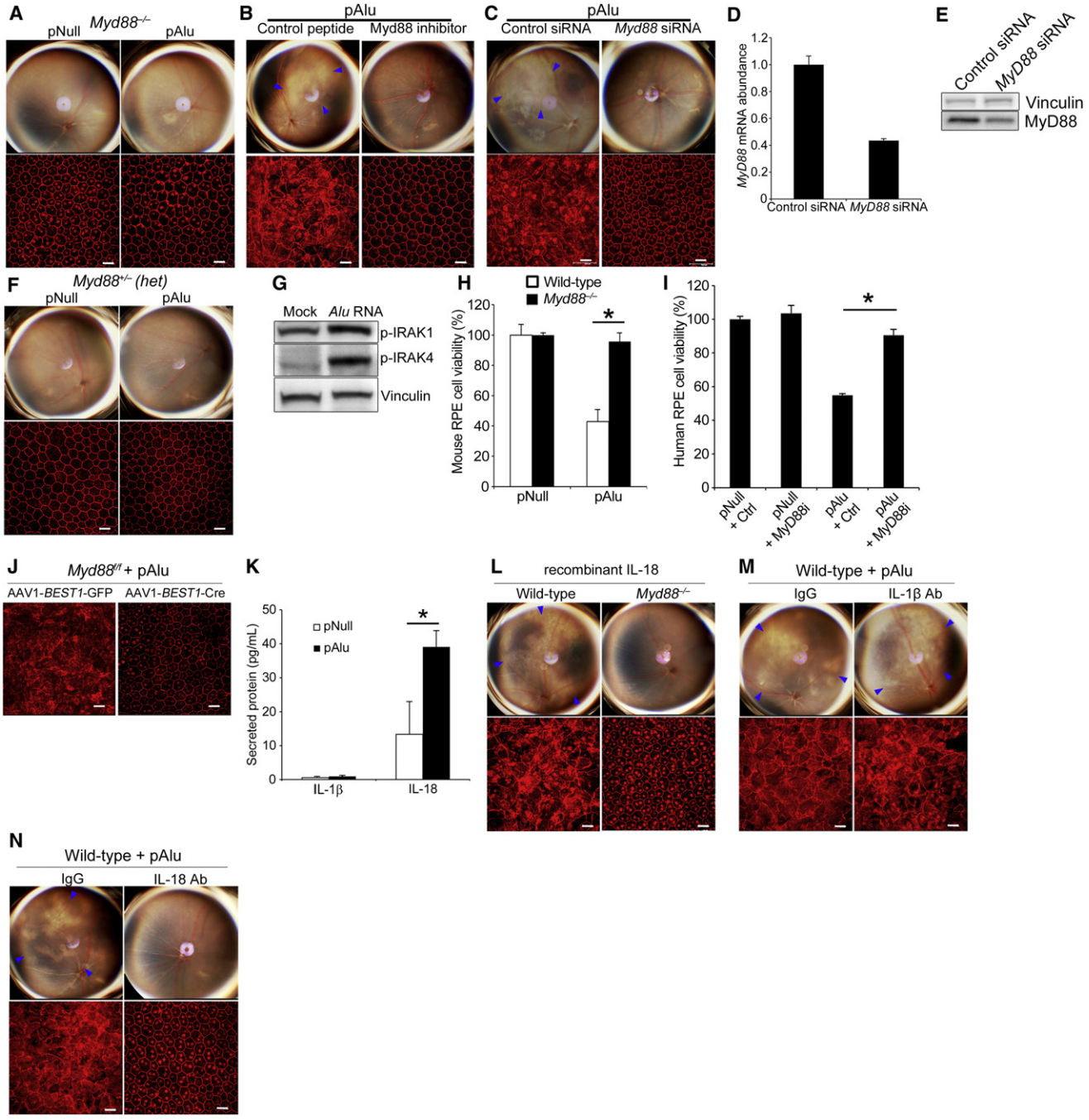

Figure 2. *Alu* RNA Induces RPE Degeneration via MyD88

(A) pAlu does not induce RPE degeneration in *Myd88*$^{-/-}$ mice.

(B) pAlu-induced RPE degeneration in WT mice is inhibited by a MyD88 homodimerization peptide inhibitor (MyD88i), but not by a control peptide.

(C) pAlu-induced RPE degeneration in WT mice is inhibited by cholesterol-conjugated *Myd88* siRNA but not control siRNA.

(D and E) siRNA targeting *MyD88* (si*MyD88*) reduces target gene (D) and protein (E) abundance in mouse RPE cells compared to control siRNA. n = 3, *p < 0.05 by Student's t test.

(F) pAlu does not induce RPE degeneration in *Myd88* heterozygous (het) mice.

(G) Western blot of *Alu* RNA-induced IRAK1 and IRAK4 phosphorylation in human RPE cells. Image representative of three experiments.

(H) pAlu reduces cell viability of WT but not *Myd88*$^{-/-}$ mouse RPE cells.

(I) Loss of human RPE cell viability induced by pAlu is rescued by MyD88i.

(J) AAV1-*BEST1*-Cre, but not AAV1-*BEST1*-GFP, protected *Myd88*$^{f/f}$ mice from pAlu-induced RPE degeneration.

(K) pAlu induces IL18 secretion from human RPE cells measured by ELISA. IL1β secretion is barely detectable. n = 3, *p < 0.05 by Student's t test.

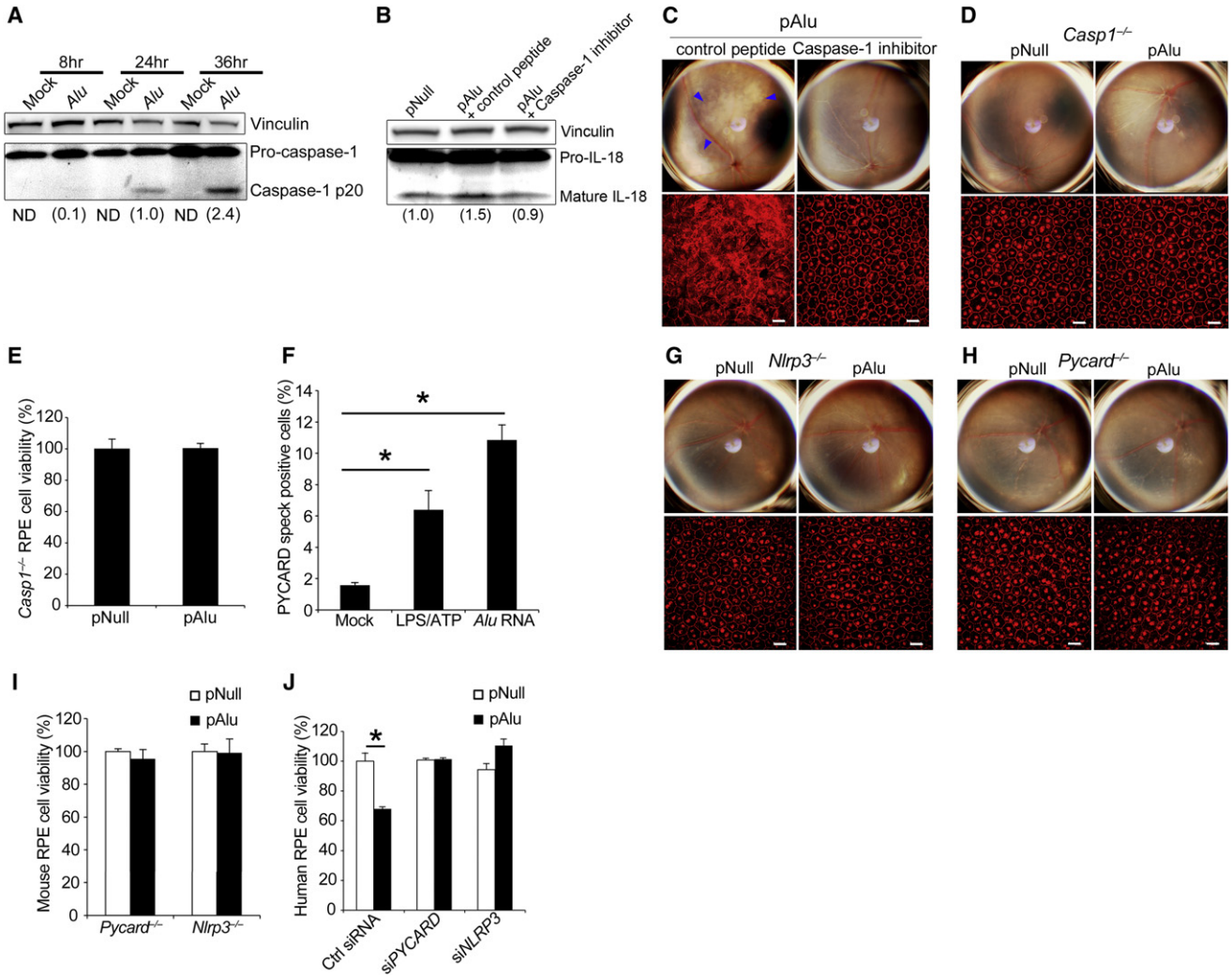

Figure 3. *Alu* RNA Induces RPE Degeneration via NLRP3 Inflammasome

(A) Western blot of Caspase-1 activation (p20 subunit) by *Alu* RNA in human RPE cells.

(B) Western blot of pAlu-induced IL18 maturation in RPE cell lysates in WT mice impaired by Caspase-1 peptide inhibitor.

(C) Caspase-1 peptide inhibitor protects WT mice from pAlu-induced RPE degeneration.

(D and E) pAlu does not induce (D) RPE degeneration in *Casp1*$^{-/-}$ mice or (E) cytotoxicity in *Casp1*$^{-/-}$ mouse RPE cells.

(F) *Alu* RNA and LPS+ATP induce formation of PYCARD clusters in human RPE cells transfected with GFP-PYCARD.

(G and H) pAlu does not induce RPE degeneration in *Nlrp3*$^{-/-}$ (G) or *Pycard*$^{-/-}$ (H) mice.

(I) *Nlrp3*$^{-/-}$ and *Pycard*$^{-/-}$ mouse RPE cells are protected against pAlu-induced loss of cell viability.

(J) siRNAs targeting *NLRP3* or *PYCARD* rescued human RPE cells from pAlu-induced cytotoxicity, compared to control siRNA.

n = 3–4, *p < 0.05 by Student's t test (F and J). Data are represented as mean ± SEM (E, F, I, and G). Images representative of three experiments. Densitometry values normalized to Vinculin are shown in parentheses (A and B). Fundus photographs, top row; ZO-1-stained (red) flat mounts, bottom row. Degeneration outlined by blue arrowheads. n = 8–12. Scale bars, 20 μm (C, D, G, and H). Representative images shown. See also Figure S3.

peptide Z-WEHD-FMK, but not a control peptide Z-FA-FMK, blocked IL18 maturation and pAlu-induced RPE degeneration in WT mice (Figures 3B and 3C). The Caspase-1-inhibitory peptide blocked *Alu* RNA-induced substrate cleavage in human RPE cells (Figure S3C), confirming its mode of action. Similarly, *Casp1*$^{-/-}$ mice treated with *Alu* RNA or pAlu did not exhibit RPE degeneration (Figures 3D and S3D). Also, pAlu did not induce cell death in *Casp1*$^{-/-}$ mouse RPE cells (Figure 3E).

(L) Recombinant IL18 induces RPE degeneration in WT but not *Myd88*$^{-/-}$ mice.

(M and N) pAlu-induced RPE degeneration in WT mice is rescued by IL18-neutralizing antibody (N) but not by IL1β-neutralizing antibody (M).

Representative images shown. n = 8–12. Fundus photographs, top row; ZO-1-stained (red) flat mounts, bottom row. Degeneration outlined by blue arrowheads. Scale bars, 20 μm (A–C, F, J, and L–N). n = 3, *p < 0.05 by Student's t test. Data are represented as mean ± SEM (D, H, I, and K).

See also Figure S2.

Caspase-1 can be activated within a multiprotein innate immune complex termed the inflammasome (Tschopp et al., 2003). The best characterized inflammasome pathway is one that is activated by binding of NLRP3 to the Caspase-1 adaptor ASC (encoded by *PYCARD*). One hallmark of inflammasome assembly is spatial clustering of PYCARD (Fernandes-Alnemri et al., 2007). In human RPE cells transfected with fluorescent-tagged PYCARD (GFP-PYCARD), *Alu* RNA induced the appearance of a brightly fluorescent cytoplasmic cluster, similar to the effect of treatment with LPS and ATP, which activates the NLRP3 inflammasome (Figures 3F and S3E) (Mariathasan et al., 2006).

Next we tested the functional relevance of NLRP3 and PYCARD to *Alu* RNA cytotoxicity. Neither pAlu nor *Alu* RNA induced RPE degeneration in either *Nlrp3*$^{-/-}$ or *Pycard*$^{-/-}$ mice (Figures 3G, 3H, S3F, and S3G), demonstrating the critical importance of the inflammasome in *Alu* RNA cytotoxicity. Also, pAlu did not induce cell death in *Nlrp3*$^{-/-}$ or *Pycard*$^{-/-}$ mouse RPE cells (Figure 3I). Moreover, knockdown of *NLRP3* or *PYCARD* by siRNAs rescued pAlu-induced human RPE cell death (Figures 3J and S3H). These findings provide direct evidence that NLRP3 activation in response to *Alu* RNA occurs in RPE cells and does not require the presence of other immune cells.

We determined that IL18 and MyD88 activation indeed were downstream of Caspase-1 activation by showing (1) that although MyD88 inhibition reduced *Alu* RNA-induced IRAK1/4 phosphorylation in human RPE cells (Figure S2E), it did not reduce *Alu* RNA-induced Caspase-1 cleavage or fluorescent substrate cleavage (Figures S3I and S3J); (2) that IL18 neutralization did not inhibit *Alu* RNA-induced Caspase-1 cleavage (Figure S3K); and (3) that Caspase-1 inhibition reduced *Alu* RNA-induced phosphorylation of IRAK1/4 (Figure S3L).

Alu RNA Induces Mitochondrial ROS and NLRP3 Priming

NLRP3 inflammasome function requires two signals, the first of which is termed priming. pAlu induced inflammasome priming as it upregulated both *NLRP3* and *IL18* mRNAs. This priming occurred equivalently in both WT and *Myd88*$^{-/-}$ mouse RPE cells (Figure 4A), further corroborating that MyD88 functions downstream of NLRP3 in this system. Akin to other inflammasome agonists that do not directly interact with NLRP3 (Tschopp and Schroder, 2010), we did not observe a physical interaction between *Alu* RNA and NLRP3 (Figure S4A). To determine how *Alu* RNA primed the inflammasome, we studied whether it induced reactive oxygen species (ROS) production, a signal for priming (Bauernfeind et al., 2011; Nakahira et al., 2011). pAlu induced ROS generation in human RPE cells (Figure 4B), and the ROS inhibitor diphenyliodonium (DPI) blocked pAlu-induced *NLRP3* and *IL18* mRNA upregulation and *Alu* RNA-induced RPE degeneration in WT mice (Figures 4C and 4D). As DPI blocks mitochondrial ROS and phagosomal ROS (Li and Trush, 1998), we tested which pathway was triggered because there is controversy surrounding the source of ROS contributing to NLRP3 responses (Latz, 2010).

We used MitoSOX Red, which labels ROS-generating mitochondria, in combination with MitoTracker Deep Red, which labels respiring mitochondria. To monitor phagosomal ROS generation, we used Fc OxyBURST Green, which measures activation of NADPH oxidase within the phagosome. A marked increase in ROS-generating mitochondria was observed in human RPE cells transfected with pAlu (Figure 4E). In contrast, whereas phorbol myristate acetate (PMA) induced phagosomal ROS as expected (Savina et al., 2006), pAlu did not do so (Figure 4F). These data are consistent with the findings that NLRP3 responses are impaired by mitochondrial ROS inhibitors (Nakahira et al., 2011; Zhou et al., 2011) but are preserved in cells carrying genetic mutations that impair NADPH-oxidase-dependent ROS production (Meissner et al., 2010; van Bruggen et al., 2010).

Consonant with these reports and the observation that the principal source of cellular ROS is mitochondria (Murphy, 2009), we found that the mitochondria-targeted antioxidants Mito-TEMPO and MitoQ (Murphy and Smith, 2007; Nakahira et al., 2011) both blocked *Alu* RNA-induced RPE degeneration in WT mice, whereas dTPP, a structural analog of MitoQ that does not scavenge mitochondrial ROS, did not do so (Figure 4G). In contrast, gp91 ds-tat, a cell-permeable peptide that inhibits association of two essential NADPH oxidase subunits (gp91^{phox} and p47^{phox}) (Rey et al., 2001), did not do so (Figure 4H). Corroborating these data, *Alu* RNA induced RPE degeneration in mice deficient in *Cybb* (which encodes gp91^{phox}) just as in WT mice (Figure 4I). Next we studied the voltage-dependent anion channels (VDAC) because *VDAC1* and *VDAC2*, but not *VDAC3*, are important in mitochondrial ROS produced by NLRP3 activators in macrophages (Zhou et al., 2011). Consistent with these observations, siRNA knockdown of *VDAC1* and *VDAC2*, but not *VDAC3*, impaired pAlu-induced mitochondrial ROS (Figures 4J and S4B) and *NLRP3* and *IL18* mRNA induction in human RPE cells (Figure 4K). Collectively, these data implicate mitochondrial ROS in *Alu* RNA-induced NLRP3 inflammasome-mediated RPE degeneration.

Alu RNA Does Not Induce RPE Degeneration via Pyroptosis

Alu RNA activates Caspase-1, which can trigger pyroptosis, a form of cell death characterized by formation of membrane pores and osmotic lysis (Fink and Cookson, 2006). The cytoprotective agent glycine, which attenuates pyroptosis (Fink et al., 2008; Fink and Cookson, 2006; Verhoef et al., 2005), inhibited human RPE cell death induced by LPS+ATP but not by *Alu* RNA (Figures 5A and 5B). Pyroptosis requires Caspase-1 but can proceed independent of IL18 (Miao et al., 2010). Thus, our finding that IL18 induced RPE degeneration in *Casp1*$^{-/-}$ mice (Figure 5C), coupled with the lack of rescue by glycine, suggests that *Alu* RNA-induced RPE degeneration does not occur via pyroptosis.

DICER1 Loss Induces Cell Death via Inflammasome

We previously demonstrated the key role of DICER1 in maintaining RPE cell health (Kaneko et al., 2011): DICER1-cleaved *Alu* RNA did not induce RPE degeneration in vivo; DICER1 overexpression protected against *Alu* RNA-induced RPE degeneration; and DICER1 loss-induced RPE degeneration was blocked by antagonizing *Alu* RNA (Kaneko et al., 2011). Also, rescue of DICER1 knockdown-induced RPE degeneration by *Alu* RNA

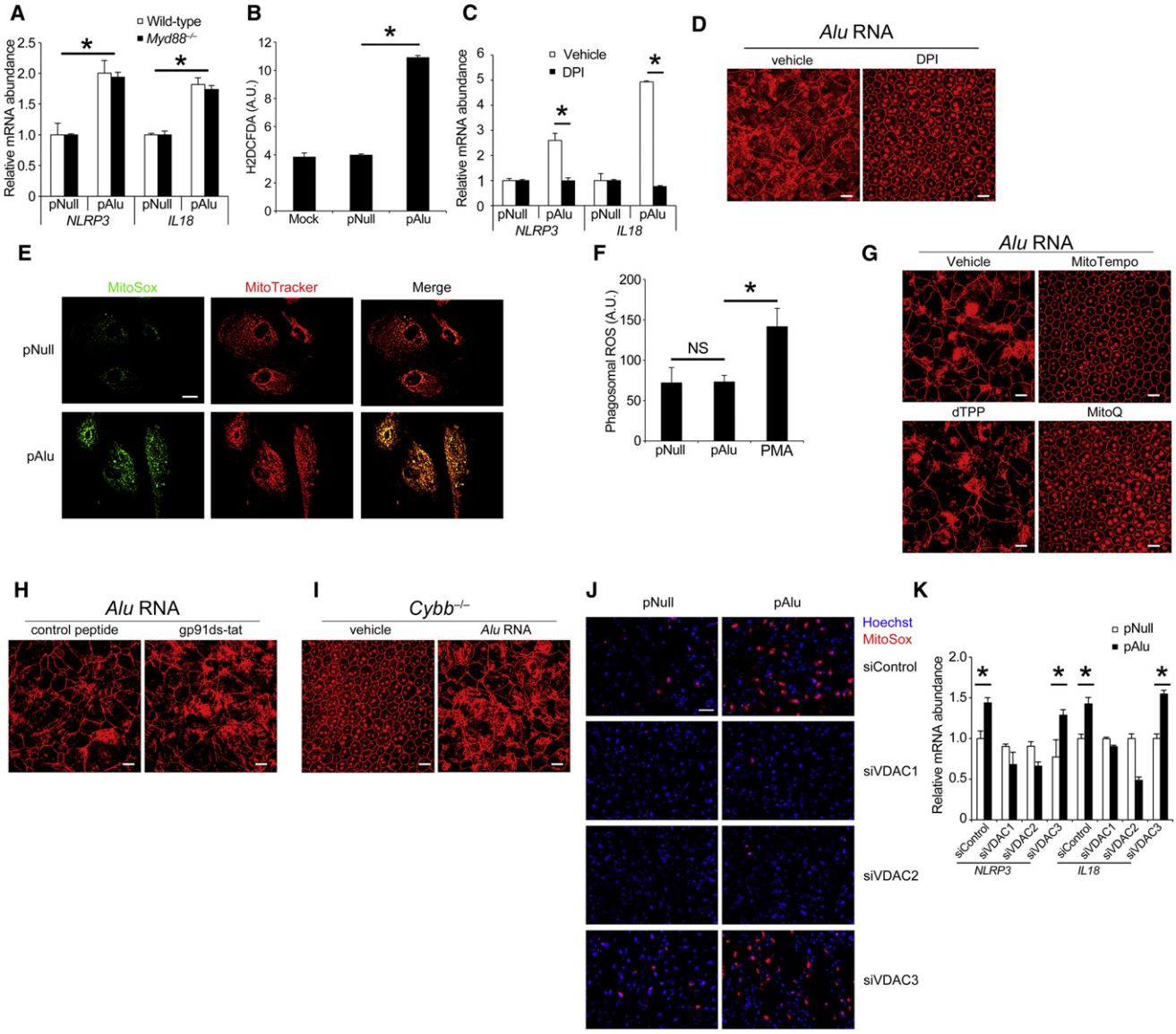

Figure 4. *Alu* RNA Induces Mitochondrial ROS Production and NLRP3 Priming

(A) pAlu induces *NLRP3* and *IL18* mRNAs in WT and *Myd88*$^{-/-}$ mouse RPE cells.

(B) pAlu induces generation of ROS in human RPE cells as monitored with the fluorescent probe H_2DCFDA (A.U., arbitrary units).

(C) DPI blocks pAlu-induced *NLRP3* and *IL18* mRNAs in human RPE cells.

(D) DPI protects WT mice from pAlu-induced RPE degeneration.

(E) pAlu induces generation of mitochondrial ROS in human RPE cells as detected by the fluorescence of MitoSOX Red (green pseudocolor), colocalized with respiring mitochondria labeled by MitoTracker Deep Red (red).

(F) PMA, but not pAlu, induces phagosomal ROS generation, as assessed by fluorescent Fc OXYBURST Green assay in human RPE cells (A.U., arbitrary units).

(G) MitoTempo and MitoQ, but not vehicle or dTPP controls, prevent *Alu* RNA-induced RPE degeneration in WT mice.

(H) NADPH oxidase inhibitor gp91 ds-tat or a scrambled peptide do not prevent *Alu* RNA-induced RPE degeneration in WT mice.

(I) *Alu* RNA induces RPE degeneration mice deficient in *Cybb* (which encodes the gp91^{phox} subunit of NADPH oxidase).

(J and K) siRNAs targeting *VDAC1* and *VDAC2*, but not *VDAC3* or scrambled control, prevent pAlu-induced mitochondrial ROS generation (J) and upregulation of *NLRP3* and *IL18* mRNAs (K) in human RPE cells. Mitochondrial ROS visualized with MitoSox Red dye and cell nuclei with Hoechst stain.

n = 3–4, *p < 0.05 by Student's t test (A–C, F, and K); NS, not significant by Student's t test (F). Data are represented as mean ± SEM (A–C, F, and K). Representative images shown; n = 8–12. ZO-1-stained (red) flat mounts. Scale bars, 20 μm (D, E, and G–I), n = 3–4. Scale bar, 100 μm (J). See also Figure S4.

inhibition was not accompanied by restoration of miRNA deficits (Kaneko et al., 2011). Therefore, we tested whether DICER1 also prevented NLRP3 inflammasome activation by *Alu* RNA. *Alu* RNA-induced Caspase-1 activation in human RPE cells was inhibited by DICER1 overexpression (Figures 6A and 6B). Conversely, Caspase-1 cleavage induced by DICER1

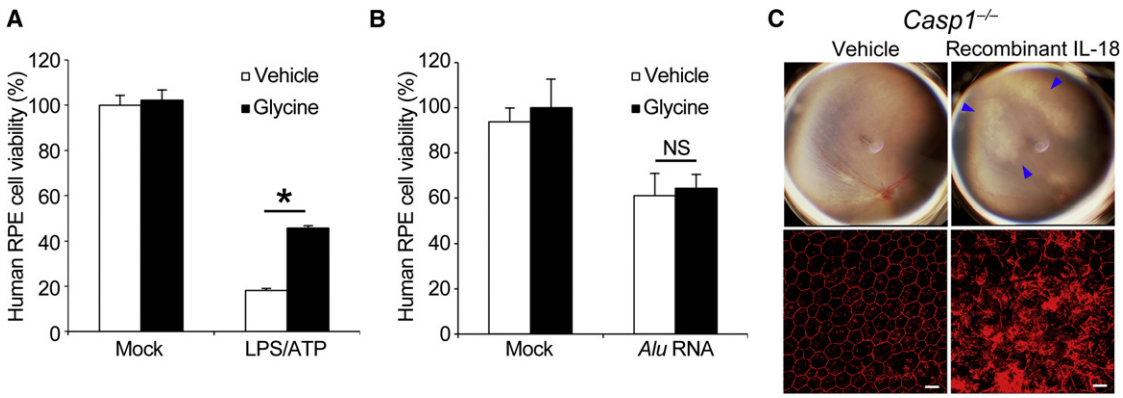

Figure 5. RPE Degeneration Does Not Occur via Pyroptosis

(A and B) Glycine inhibits human RPE cell death induced by LPS+ATP (A) but not by pAlu (B).

(C) Recombinant IL18 induces RPE degeneration in *Casp1*$^{-/-}$ mice.

n = 3–4 (A and B), *p < 0.05 by Student's t test. Data are represented as mean ± SEM (A and B). Representative images shown. n = 8–12. Fundus photographs, top row; ZO-1-stained (red) flat mounts, bottom row. Degeneration outlined by blue arrowheads. Scale bars, 20 μm (C).

knockdown in human RPE cells was inhibited by simultaneous antisense knockdown of *Alu* RNA (Figures S5A and S5B).

Next we tested the relevance of these pathways in the context of DICER1 loss in vivo. Caspase-1 cleavage was increased in the RPE of *BEST1 Cre*; *Dicer1*$^{f/f}$ mice (Figure 6C), which lose DICER1 expression in the RPE during development and exhibit RPE degeneration (Kaneko et al., 2011). Subretinal delivery of AAV1-*BEST1*-Cre in *Dicer1*$^{f/f}$ mice induced Caspase-1 activation and IL18 maturation in the RPE (Figure 6D). This treatment also induced RPE degeneration, which was blocked by intravitreous delivery of the Caspase-1-inhibitory peptide but not the control peptide (Figure 6E). AAV1-*BEST1*-Cre-induced RPE degeneration in *Dicer1*$^{f/f}$ mice was also blocked by intravitreous delivery of the MyD88-inhibitory peptide but not a control peptide (Figure 6F). In addition, MyD88 inhibition prevented cell death in human RPE cells treated with antisense oligonucleotides targeting *DICER1* (Figure 6G). *DICER1* knockdown in human RPE cells increased IRAK1/4 phosphorylation, providing further evidence of MyD88 activation upon loss of DICER1 (Figure 6H). MyD88 inhibition also prevented cell death in *Dicer1*$^{f/f}$ mouse RPE cells treated with an adenoviral vector coding for Cre recombinase (Figure 6I). MyD88 inhibition blocked RPE cell death without restoring the miRNA expression deficits induced by *Dicer1* knockdown (Figure 6J). These findings demonstrate that DICER1 is an essential endogenous negative regulator of NLRP3 inflammasome activation, and that DICER1 deficiency leads to *Alu* RNA-mediated, MyD88-dependent, miRNA-independent RPE degeneration.

Inflammasome and MyD88 Activation in Human GA

Next we tested whether human eyes with GA, which exhibit loss of DICER1 and accumulation of *Alu* RNA in their RPE (Kaneko et al., 2011), also display evidence of inflammasome activation. The abundance of *NLRP3* mRNA in the RPE of human eyes with GA was markedly increased compared to control eyes (Figure 7A). *IL18* and *IL1B* mRNA abundance also was increased in GA RPE; however, only the disparity in *IL18* levels reached statistical significance (Figure 7A). Immunolocalization studies showed that the expression of NLRP3, PYCARD, and Caspase-1 proteins was also increased in GA RPE (Figures 7B–7D). Western blot analyses corroborated the increased abundance of NLRP3 and PYCARD in GA RPE and revealed greatly increased levels of the enzymatically active cleaved Caspase-1 p20 subunit in GA RPE (Figure 7E). There was also an increase in the abundance of phosphorylated IRAK1 and IRAK4 in GA RPE, indicative of increased MyD88 signal transduction (Figure 7E). Collectively, these data provide evidence of NLRP3 inflammasome and MyD88 activation in situ in human GA, mirroring the functional data in human RPE cell culture and mice in vivo.

DISCUSSION

Our data establish a functional role for the subversion of innate immune sensing pathways by *Alu* RNA in the pathogenesis of GA. Collectively, our findings demonstrate that the NLRP3 inflammasome senses GA-associated *Alu* RNA danger signals and contributes to RPE degeneration and potentially vision loss in AMD (Figure S6). To date, the function of the NLRP3 inflammasome has been largely restricted to immune cells in vivo. Our finding that it plays a critical function in RPE cell survival broadens the cellular scope of this inflammasome and raises the possibility that other nonimmune cells could employ this platform.

The NLRP3 inflammasome was originally recognized as a sensor of external danger signals such as microbial toxins (Kanneganti et al., 2006; Mariathasan et al., 2006; Muruve et al., 2008). Subsequently, endogenous crystals, polypeptides, and lipids were reported to activate it in diseases such as gout, atherogenesis, Alzheimer's disease, and type 2 diabetes (Halle et al., 2008; Masters et al., 2010; Muruve et al., 2008; Wen et al., 2011). To our knowledge, *Alu* RNA is the first endogenous nucleic acid known to activate this immune platform. Our findings expand the diversity of endogenous danger signals in

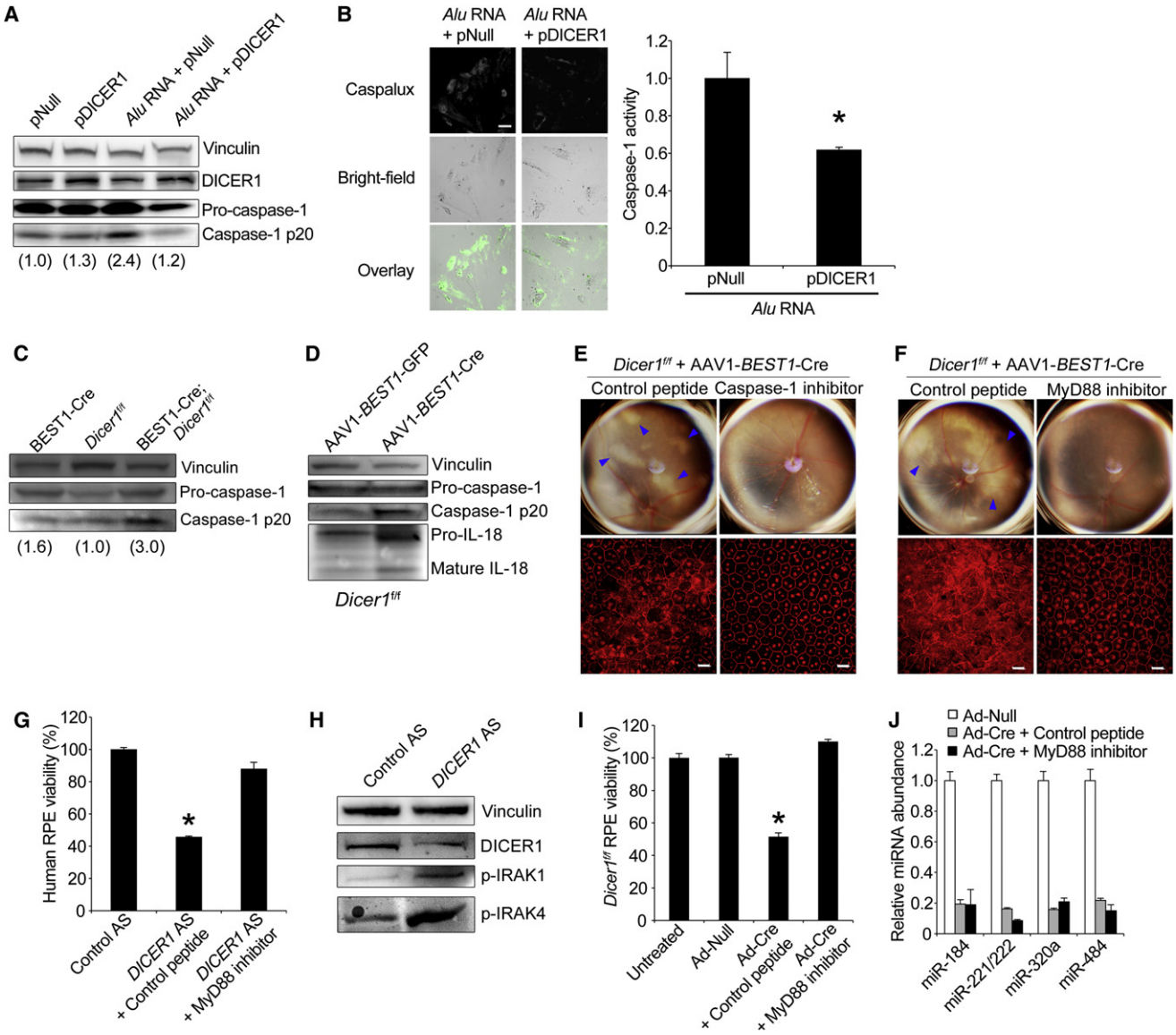

Figure 6. DICER1 Loss Induces Cell Death via Inflammasome

(A) Western blot of *Alu* RNA-induced Caspase-1 cleavage (p20) inhibited by DICER1 overexpression in human RPE cells.

(B and C) DICER1 overexpression reduces *Alu* RNA-induced Caspase-1 activation in human RPE cells (measured by cleavage [B, left panel, green] of Caspalux1 fluorescent substrate). Fluorescence quantification shown in right panel.

(C) Western blot of increased Caspase-1 activation (p20 subunit) in RPE cell lysates of *BEST1-Cre*; *Dicer1*$^{f/f}$ mice compared to *BEST1-Cre* or *Dicer1*$^{f/f}$ mice.

(D) Western blot of increased Caspase-1 activation (p20 subunit) and IL18 maturation in RPE cell lysates of *Dicer1*$^{f/f}$ mice treated with AAV1-*BEST1*-Cre.

(E and F) RPE degeneration induced by AAV1-*BEST1*-Cre in *Dicer1*$^{f/f}$ mice is rescued by peptide inhibitors of either Caspase-1 (E) or MyD88 (F).

(G) MyD88 inhibitor rescues loss of human RPE cell viability induced by DICER1 antisense (AS) treatment.

(H) *DICER1* antisense (AS) treatment of human RPE cells reduces DICER1 and increases IRAK1 and IRAK4 phosphorylation.

(I) MyD88 inhibitor rescues loss of cell viability in *Dicer1*$^{f/f}$ mouse RPE cells treated with adenoviral vector coding for Cre recombinase (Ad-Cre).

(J) Ad-Cre induced global miRNA expression deficits in *Dicer1*$^{f/f}$ mouse RPE cells compared to Ad-Null. No significant difference was found in miRNA abundance between MyD88 inhibitor and control peptide-treated Dicer1 depleted cells.

n = 3 (A, B, and F–H). Images are representative of three experiments (A, C, D, and H). Densitometry values normalized to Vinculin are shown in parentheses (A and C). n = 3–4, *$p < 0.05$ by Student's t test. Data are represented as mean ± SEM (B, G, and I). Representative images shown. n = 8–12. ZO-1-stained (red) flat mounts. Scale bars, 20 μm (E and F). See also Figure S5.

chronic human diseases and comport with the concept that this inflammasome is a sensor of metabolic danger (Schroder et al., 2010).

Dampening inflammasome activation can be essential to limiting the inflammatory response. Pathogens have evolved many strategies to inhibit inflammasome activation (Martinon

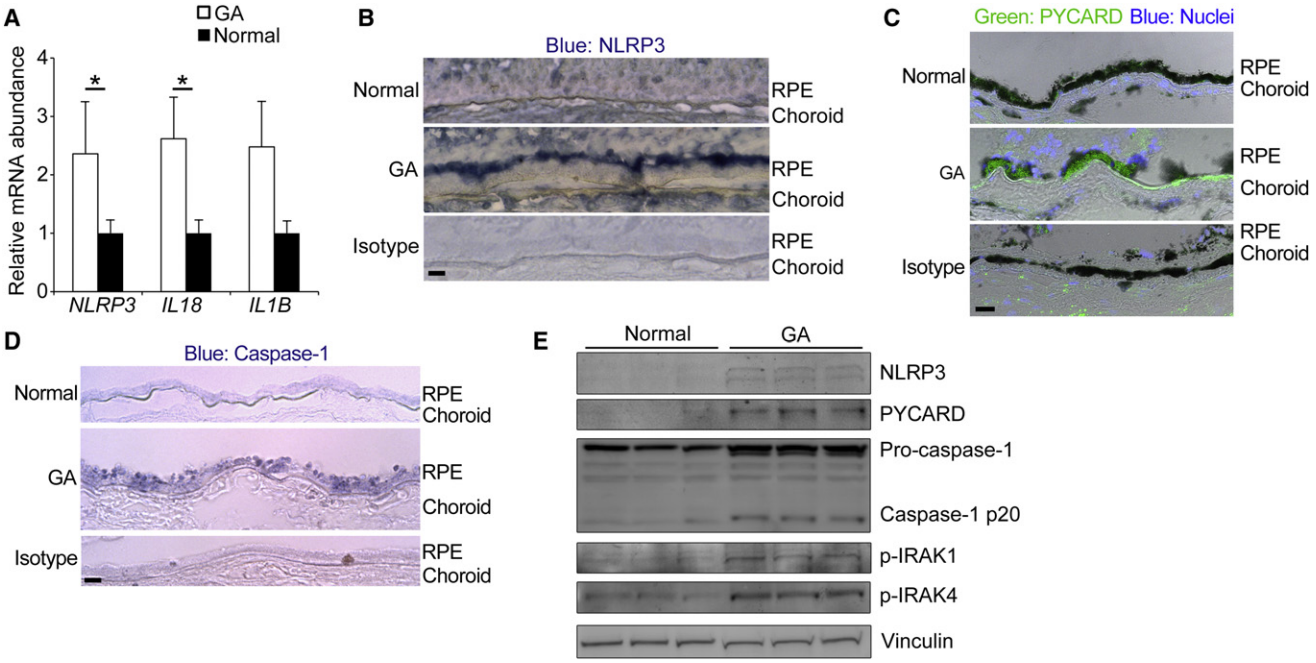

Figure 7. NLRP3 Inflammasome and MyD88 Activation in Human GA

(A) *NLRP3* and *IL18* abundance was significantly elevated in macular GA RPE (n = 13) compared to normal age-matched controls (n = 12). *$p < 0.05$ by Mann-Whitney U test. There was no significant difference between groups ($p = 0.32$ by Mann-Whitney U test) in *IL1B* abundance.

(B–D) Increased immunolocalization of NLRP3 (B), PYCARD (C), and Caspase-1 (D) in macular GA RPE compared to age-matched normal controls. Scale bars, 20 μm.

(E) Western blots of macular RPE lysates from individual human donor eyes show that abundance of NLRP3, PYCARD, and phosphorylated IRAK1/4, normalized to the levels of the housekeeping protein Vinculin, is increased in GA compared to age-matched normal controls.

Data are represented as mean ± SEM (A). Representative images shown. n = 6 (B–E). See also Figure S6.

et al., 2009). Likewise, host autophagy proteins (Nakahira et al., 2011), type I interferon (Guarda et al., 2011), and T cell contact with macrophages can inhibit this process (Guarda et al., 2009). Our finding that DICER1, through its cleavage of *Alu* RNA, prevents activation of NLRP3 adds to the repertoire of host inflammasome modulation capabilities and reveals a new facet of how dysregulation of homeostatic anti-inflammatory mechanisms can promote AMD (Ambati et al., 2003; Takeda et al., 2009).

Added to its recently described antiapoptotic and tumor-related functions, DICER1 emerges as a multifaceted protein. It remains to be determined how this functional versatility is channeled in various states. As DICER1 dysregulation is increasingly recognized in several human diseases, it is reasonable to imagine that *Alu* RNA might be an inflammasome activating danger signals in those conditions too. It is also interesting that, at least in adult mice and in a variety of mouse and human cells, the miRNA biogenesis function of DICER1 is not critical for cell survival, at least in a MyD88-deficient environment (data not shown).

Our data that mitochondrial ROS production is involved in *Alu* RNA-induced RPE degeneration comport with observations of mitochondrial DNA damage (Lin et al., 2011), downregulation of proteins involved in mitochondrial energy production and trafficking (Nordgaard et al., 2008), and reduction in the number and size of mitochondria (Feher et al., 2006) in the RPE of human eyes with AMD. Jointly, these findings suggest a potential therapeutic benefit to interfering with mitochondrial ROS generation.

Current clinical programs targeting the inflammasome largely focus on IL1β; presently there are no IL18 inhibitors in registered clinical trials. However, our data indicate that IL18 is more important than IL1β in mediating RPE cell death in GA (similar to selective IL18 involvement in a colitis model; Zaki et al., 2010), pointing to the existence of regulatory mechanisms by which inflammasome activation bifurcates at the level of or just preceding the interleukin effectors. Although Caspase-1 inhibition could be an attractive local therapeutic strategy, caspase inhibitors can promote alternative cell death pathways, possibly limiting their utility (Vandenabeele et al., 2006).

MyD88 is best known for transducing TLR signaling initiated by pathogen-associated molecular patterns (O'Neill and Bowie, 2007), although recently it has been implicated in human cancers (Ngo et al., 2011; Puente et al., 2011). Our findings introduce an unexpected function for MyD88 in effecting death signals from mobile element transcripts that can lead to retinal degeneration and blindness and raise the possibility that MyD88 could be a central integrator of signals from other non-NLRP3 inflammasomes that also employ Caspase-1 (Schroder and Tschopp, 2010). Because noncanonical activation of MyD88 is a critical checkpoint in RPE degeneration in GA (Figure S6), it represents an enticing therapeutic target. A potential concern is its important antimicrobial function in mice (O'Neill and Bowie, 2007).

However, in contrast to *Myd88*$^{-/-}$ mice, adult humans with MyD88 deficiency are described to be generally healthy and resistant to a wide variety of microbial pathogens (von Bernuth et al., 2008). MyD88-deficient humans have a narrow susceptibility range to pyogenic bacterial infections, and that too only in early childhood and not adult life (Picard et al., 2010). Moreover, as evident from the siRNA and *Myd88*$^{+/-}$ studies, partial inhibition of MyD88 is sufficient to protect against *Alu* RNA. Localized intraocular therapy, the current standard of care in most retinal diseases, would further limit the likelihood of adverse infectious outcomes. It is reasonable to foresee development of MyD88 inhibitors for prevention or treatment of GA.

EXPERIMENTAL PROCEDURES

A detailed description of materials and methods can be found in the Extended Experimental Procedures.

Subretinal Injection and Imaging

Subretinal injections (1 μl) were performed using a Pico-Injector (PLI-100, Harvard Apparatus). Plasmids were transfected in vivo using 10% Neuroporter (Genlantis). Fundus imaging was performed on a TRC-50 IX camera (Topcon) linked to a digital imaging system (Sony). RPE flat mounts were immunolabeled using antibodies against zonula occludens-1 (Invitrogen).

Cell Viability

Cell viability was assessed using CellTiter 96 AQueous One Solution Cell Proliferation Assay (Promega) according to manufacturer's instructions.

mRNA Abundance

Transcript abundance was quantified by real-time RT-PCR using an Applied Biosystems 7900 HT Fast Real-Time PCR system by the $2^{-\Delta\Delta Ct}$ method.

Protein Abundance and Activity

Protein abundance was assessed by western blot analysis using antibodies against Caspase-1 (1:500; Invitrogen), pIRAK1 (1:500, Thermo Scientific), pIRAK4 (1:500, Abbomax), PYCARD (1:200, Santa Cruz Biotechnology), NLRP3 (1:500, Enzo Life Sciences), and Vinculin (1:1,000, Sigma-Aldrich). Caspase-1 activity was visualized using Caspalux1 E1D2 (OncoImmunin) according to manufacturer's instructions.

Statistical Analysis

Results are expressed as mean ± standard error of the mean (SEM), with p values < 0.05 considered statistically significant. Differences between groups were compared by Mann-Whitney U test or Student's t test, as appropriate, and two-tailed p values are reported.

SUPPLEMENTAL INFORMATION

Supplemental Information includes Extended Experimental Procedures and six figures and can be found with this article online at doi:10.1016/j.cell.2012.03.036.

ACKNOWLEDGMENTS

We thank S. Akira, Z. Chen, M. Chrenek, J. Garcia-Perez, T. Heidmann, and J.V. Moran for providing mice, reagents, or tissues; R. King, L. Xu, M. McConnell, C. Payne, D. Robertson, G. Botzet, G.R. Pattison, and C. Spee for technical assistance; and S. Bondada, M.E. Boulton, R.A. Brekken, R. Kannan, K. Karikó, T.S. Khurana, R. Mohan, M.L. Peterson, V. Rangnekar, A. Sinai, A.M. Rao, G.S. Rao, and K. Ambati for discussions. J.A. was supported by NEI/NIH grants R01EY018350, R01EY018836, R01EY020672, R01EY022238, R21EY019778, and RC1EY020442, Doris Duke Distinguished Clinical Scientist Award, Burroughs Wellcome Fund Clinical Scientist Award in Translational Research, Dr. E. Vernon Smith and Eloise C. Smith Macular Degeneration Endowed Chair, and Senior Scientist Investigator Award (Research to Prevent Blindness, RPB); J.Z.B. by NIH K08EY021521, International Retinal Research Foundation, and American Health Assistance Foundation; M.E.K. by NIH K08EY021757; B.J.F., S.B., and M.E.K. by NIH T32HL091812 and UL1RR033173; G.N. by NIH R01AI063331 and R01AR052756; Y.H. by Alcon Japan Research award; W.W.H. by NIH P30EY021721; B.K.A. by NIH R01EY017182 and R01EY017950, VA Merit Award, and Department of Defense; D.R.H. by NIH P30EY003040 and R01EY001545; J.F.K. and J.A.G. by NIH R01GM068414; J.W.Y. and D.-k.L. by Global Research Laboratory grant from MEST, Korea. Departmental unrestricted grants from RPB supported J.A. and W.W.H. University of Kentucky Physician Scientist Awards supported J.Z.B. and M.E.K. P.P. is a Senior Scholar from the Fonds de la Recherche en Santé du Québec (FRSQ). Several authors are named as inventors on patent applications filed by their universities relating to described technologies. V.T., Y.H., B.D.G., S.D., Y.K., W.G.C., J.Z.B., H.K., N.K., B.J.F., S.B., and M.E.K. performed experiments. W.W.H., V.A.C, S.L.P., J.F.K., J.A.G., M.P.M., J.W.Y., D.-k.L, D.R.H., P.P., and G.N. provided reagents. J.A. conceived and directed the project and wrote the paper with assistance from B.K.A., B.J.F., and B.D.G. All authors had the opportunity to discuss the results and comment on the manuscript.

Received: October 7, 2011
Revised: February 19, 2012
Accepted: March 26, 2012
Published online: April 26, 2012

REFERENCES

Adachi, O., Kawai, T., Takeda, K., Matsumoto, M., Tsutsui, H., Sakagami, M., Nakanishi, K., and Akira, S. (1998). Targeted disruption of the MyD88 gene results in loss of IL-1- and IL-18-mediated function. Immunity *9*, 143–150.

Akira, S., Uematsu, S., and Takeuchi, O. (2006). Pathogen recognition and innate immunity. Cell *124*, 783–801.

Alexopoulou, L., Holt, A.C., Medzhitov, R., and Flavell, R.A. (2001). Recognition of double-stranded RNA and activation of NF-kappaB by Toll-like receptor 3. Nature *413*, 732–738.

Allensworth, J.J., Planck, S.R., Rosenbaum, J.T., and Rosenzweig, H.L. (2011). Investigation of the differential potentials of TLR agonists to elicit uveitis in mice. J. Leukoc. Biol. *90*, 1159–1166.

Ambati, J., Ambati, B.K., Yoo, S.H., Ianchulev, S., and Adamis, A.P. (2003). Age-related macular degeneration: etiology, pathogenesis, and therapeutic strategies. Surv. Ophthalmol. *48*, 257–293.

Batzer, M.A., and Deininger, P.L. (2002). Alu repeats and human genomic diversity. Nat. Rev. Genet. *3*, 370–379.

Bauernfeind, F., Bartok, E., Rieger, A., Franchi, L., Núñez, G., and Hornung, V. (2011). Cutting edge: reactive oxygen species inhibitors block priming, but not activation, of the NLRP3 inflammasome. J. Immunol. *187*, 613–617.

Bernstein, E., Caudy, A.A., Hammond, S.M., and Hannon, G.J. (2001). Role for a bidentate ribonuclease in the initiation step of RNA interference. Nature *409*, 363–366.

Blaauwgeers, H.G., Holtkamp, G.M., Rutten, H., Witmer, A.N., Koolwijk, P., Partanen, T.A., Alitalo, K., Kroon, M.E., Kijlstra, A., van Hinsbergh, V.W., and Schlingemann, R.O. (1999). Polarized vascular endothelial growth factor secretion by human retinal pigment epithelium and localization of vascular endothelial growth factor receptors on the inner choriocapillaris. Evidence for a trophic paracrine relation. Am. J. Pathol. *155*, 421–428.

Cao, Z., Henzel, W.J., and Gao, X. (1996). IRAK: a kinase associated with the interleukin-1 receptor. Science *271*, 1128–1131.

Diebold, S.S., Kaisho, T., Hemmi, H., Akira, S., and Reis e Sousa, C. (2004). Innate antiviral responses by means of TLR7-mediated recognition of single-stranded RNA. Science *303*, 1529–1531.

Feher, J., Kovacs, I., Artico, M., Cavallotti, C., Papale, A., and Balacco Gabrieli, C. (2006). Mitochondrial alterations of retinal pigment epithelium in age-related macular degeneration. Neurobiol. Aging *27*, 983–993.

Feldmeyer, L., Keller, M., Niklaus, G., Hohl, D., Werner, S., and Beer, H.D. (2007). The inflammasome mediates UVB-induced activation and secretion of interleukin-1beta by keratinocytes. Curr. Biol. *17*, 1140–1145.

Fernandes-Alnemri, T., Wu, J., Yu, J.W., Datta, P., Miller, B., Jankowski, W., Rosenberg, S., Zhang, J., and Alnemri, E.S. (2007). The pyroptosome: a supramolecular assembly of ASC dimers mediating inflammatory cell death via caspase-1 activation. Cell Death Differ. *14*, 1590–1604.

Fink, S.L., Bergsbaken, T., and Cookson, B.T. (2008). Anthrax lethal toxin and Salmonella elicit the common cell death pathway of caspase-1-dependent pyroptosis via distinct mechanisms. Proc. Natl. Acad. Sci. USA *105*, 4312–4317.

Fink, S.L., and Cookson, B.T. (2006). Caspase-1-dependent pore formation during pyroptosis leads to osmotic lysis of infected host macrophages. Cell. Microbiol. *8*, 1812–1825.

Ghayur, T., Banerjee, S., Hugunin, M., Butler, D., Herzog, L., Carter, A., Quintal, L., Sekut, L., Talanian, R., Paskind, M., et al. (1997). Caspase-1 processes IFN-gamma-inducing factor and regulates LPS-induced IFN-gamma production. Nature *386*, 619–623.

Gu, Y., Kuida, K., Tsutsui, H., Ku, G., Hsiao, K., Fleming, M.A., Hayashi, N., Higashino, K., Okamura, H., Nakanishi, K., et al. (1997). Activation of interferon-gamma inducing factor mediated by interleukin-1beta converting enzyme. Science *275*, 206–209.

Guarda, G., Braun, M., Staehli, F., Tardivel, A., Mattmann, C., Förster, I., Farlik, M., Decker, T., Du Pasquier, R.A., Romero, P., and Tschopp, J. (2011). Type I interferon inhibits interleukin-1 production and inflammasome activation. Immunity *34*, 213–223.

Guarda, G., Dostert, C., Staehli, F., Cabalzar, K., Castillo, R., Tardivel, A., Schneider, P., and Tschopp, J. (2009). T cells dampen innate immune responses through inhibition of NLRP1 and NLRP3 inflammasomes. Nature *460*, 269–273.

Halle, A., Hornung, V., Petzold, G.C., Stewart, C.R., Monks, B.G., Reinheckel, T., Fitzgerald, K.A., Latz, E., Moore, K.J., and Golenbock, D.T. (2008). The NALP3 inflammasome is involved in the innate immune response to amyloid-beta. Nat. Immunol. *9*, 857–865.

Heil, F., Hemmi, H., Hochrein, H., Ampenberger, F., Kirschning, C., Akira, S., Lipford, G., Wagner, H., and Bauer, S. (2004). Species-specific recognition of single-stranded RNA via toll-like receptor 7 and 8. Science *303*, 1526–1529.

Hoebe, K., Du, X., Georgel, P., Janssen, E., Tabeta, K., Kim, S.O., Goode, J., Lin, P., Mann, N., Mudd, S., et al. (2003). Identification of Lps2 as a key transducer of MyD88-independent TIR signalling. Nature *424*, 743–748.

Hornung, V., Ellegast, J., Kim, S., Brzózka, K., Jung, A., Kato, H., Poeck, H., Akira, S., Conzelmann, K.K., Schlee, M., et al. (2006). 5′-Triphosphate RNA is the ligand for RIG-I. Science *314*, 994–997.

Kanakaraj, P., Ngo, K., Wu, Y., Angulo, A., Ghazal, P., Harris, C.A., Siekierka, J.J., Peterson, P.A., and Fung-Leung, W.P. (1999). Defective interleukin (IL)-18-mediated natural killer and T helper cell type 1 responses in IL-1 receptor-associated kinase (IRAK)-deficient mice. J. Exp. Med. *189*, 1129–1138.

Kaneko, H., Dridi, S., Tarallo, V., Gelfand, B.D., Fowler, B.J., Cho, W.G., Kleinman, M.E., Ponicsan, S.L., Hauswirth, W.W., Chiodo, V.A., et al. (2011). DICER1 deficit induces Alu RNA toxicity in age-related macular degeneration. Nature *471*, 325–330.

Kanneganti, T.D., Ozören, N., Body-Malapel, M., Amer, A., Park, J.H., Franchi, L., Whitfield, J., Barchet, W., Colonna, M., Vandenabeele, P., et al. (2006). Bacterial RNA and small antiviral compounds activate caspase-1 through cryopyrin/Nalp3. Nature *440*, 233–236.

Kato, H., Takeuchi, O., Sato, S., Yoneyama, M., Yamamoto, M., Matsui, K., Uematsu, S., Jung, A., Kawai, T., Ishii, K.J., et al. (2006). Differential roles of MDA5 and RIG-I helicases in the recognition of RNA viruses. Nature *441*, 101–105.

Keller, M., Rüegg, A., Werner, S., and Beer, H.D. (2008). Active caspase-1 is a regulator of unconventional protein secretion. Cell *132*, 818–831.

Kleinman, M.E., Kaneko, H., Cho, W.G., Dridi, S., Fowler, B.J., Blandford, A.D., Albuquerque, R.J., Hirano, Y., Terasaki, H., Kondo, M., et al. (2012). Short-interfering RNAs induce retinal degeneration via TLR3 and IRF3. Mol. Ther. *20*, 101–108.

Kleinman, M.E., Yamada, K., Takeda, A., Chandrasekaran, V., Nozaki, M., Baffi, J.Z., Albuquerque, R.J., Yamasaki, S., Itaya, M., Pan, Y., et al. (2008). Sequence- and target-independent angiogenesis suppression by siRNA via TLR3. Nature *452*, 591–597.

Kumar, H., Kawai, T., Kato, H., Sato, S., Takahashi, K., Coban, C., Yamamoto, M., Uematsu, S., Ishii, K.J., Takeuchi, O., and Akira, S. (2006). Essential role of IPS-1 in innate immune responses against RNA viruses. J. Exp. Med. *203*, 1795–1803.

Kumar, M.V., Nagineni, C.N., Chin, M.S., Hooks, J.J., and Detrick, B. (2004). Innate immunity in the retina: Toll-like receptor (TLR) signaling in human retinal pigment epithelial cells. J. Neuroimmunol. *153*, 7–15.

Lander, E.S., Linton, L.M., Birren, B., Nusbaum, C., Zody, M.C., Baldwin, J., Devon, K., Dewar, K., Doyle, M., FitzHugh, W., et al; International Human Genome Sequencing Consortium. (2001). Initial sequencing and analysis of the human genome. Nature *409*, 860–921.

Latz, E. (2010). NOX-free inflammasome activation. Blood *116*, 1393–1394.

Li, Y., and Trush, M.A. (1998). Diphenyleneiodonium, an NAD(P)H oxidase inhibitor, also potently inhibits mitochondrial reactive oxygen species production. Biochem. Biophys. Res. Commun. *253*, 295–299.

Lin, H., Xu, H., Liang, F.Q., Liang, H., Gupta, P., Havey, A.N., Boulton, M.E., and Godley, B.F. (2011). Mitochondrial DNA damage and repair in RPE associated with aging and age-related macular degeneration. Invest. Ophthalmol. Vis. Sci. *52*, 3521–3529.

Loiarro, M., Sette, C., Gallo, G., Ciacci, A., Fantò, N., Mastroianni, D., Carminati, P., and Ruggiero, V. (2005). Peptide-mediated interference of TIR domain dimerization in MyD88 inhibits interleukin-1-dependent activation of NF-κB. J. Biol. Chem. *280*, 15809–15814.

Lopez, P.F., Sippy, B.D., Lambert, H.M., Thach, A.B., and Hinton, D.R. (1996). Transdifferentiated retinal pigment epithelial cells are immunoreactive for vascular endothelial growth factor in surgically excised age-related macular degeneration-related choroidal neovascular membranes. Invest. Ophthalmol. Vis. Sci. *37*, 855–868.

Mariathasan, S., Weiss, D.S., Newton, K., McBride, J., O'Rourke, K., Roose-Girma, M., Lee, W.P., Weinrauch, Y., Monack, D.M., and Dixit, V.M. (2006). Cryopyrin activates the inflammasome in response to toxins and ATP. Nature *440*, 228–232.

Martinon, F., Mayor, A., and Tschopp, J. (2009). The inflammasomes: guardians of the body. Annu. Rev. Immunol. *27*, 229–265.

Masters, S.L., Dunne, A., Subramanian, S.L., Hull, R.L., Tannahill, G.M., Sharp, F.A., Becker, C., Franchi, L., Yoshihara, E., Chen, Z., et al. (2010). Activation of the NLRP3 inflammasome by islet amyloid polypeptide provides a mechanism for enhanced IL-1β in type 2 diabetes. Nat. Immunol. *11*, 897–904.

McLeod, D.S., Grebe, R., Bhutto, I., Merges, C., Baba, T., and Lutty, G.A. (2009). Relationship between RPE and choriocapillaris in age-related macular degeneration. Invest. Ophthalmol. Vis. Sci. *50*, 4982–4991.

Meissner, F., Seger, R.A., Moshous, D., Fischer, A., Reichenbach, J., and Zychlinsky, A. (2010). Inflammasome activation in NADPH oxidase defective mononuclear phagocytes from patients with chronic granulomatous disease. Blood *116*, 1570–1573.

Miao, E.A., Leaf, I.A., Treuting, P.M., Mao, D.P., Dors, M., Sarkar, A., Warren, S.E., Wewers, M.D., and Aderem, A. (2010). Caspase-1-induced pyroptosis is an innate immune effector mechanism against intracellular bacteria. Nat. Immunol. *11*, 1136–1142.

Murphy, M.P. (2009). How mitochondria produce reactive oxygen species. Biochem. J. *417*, 1–13.

Murphy, M.P., and Smith, R.A. (2007). Targeting antioxidants to mitochondria by conjugation to lipophilic cations. Annu. Rev. Pharmacol. Toxicol. *47*, 629–656.

Muruve, D.A., Pétrilli, V., Zaiss, A.K., White, L.R., Clark, S.A., Ross, P.J., Parks, R.J., and Tschopp, J. (2008). The inflammasome recognizes cytosolic microbial and host DNA and triggers an innate immune response. Nature *452*, 103–107.

Muzio, M., Ni, J., Feng, P., and Dixit, V.M. (1997). IRAK (Pelle) family member IRAK-2 and MyD88 as proximal mediators of IL-1 signaling. Science *278*, 1612–1615.

Nakahira, K., Haspel, J.A., Rathinam, V.A., Lee, S.J., Dolinay, T., Lam, H.C., Englert, J.A., Rabinovitch, M., Cernadas, M., Kim, H.P., et al. (2011). Autophagy proteins regulate innate immune responses by inhibiting the release of mitochondrial DNA mediated by the NALP3 inflammasome. Nat. Immunol. *12*, 222–230.

Ngo, V.N., Young, R.M., Schmitz, R., Jhavar, S., Xiao, W., Lim, K.H., Kohlhammer, H., Xu, W., Yang, Y., Zhao, H., et al. (2011). Oncogenically active MYD88 mutations in human lymphoma. Nature *470*, 115–119.

Nordgaard, C.L., Karunadharma, P.P., Feng, X., Olsen, T.W., and Ferrington, D.A. (2008). Mitochondrial proteomics of the retinal pigment epithelium at progressive stages of age-related macular degeneration. Invest. Ophthalmol. Vis. Sci. *49*, 2848–2855.

O'Neill, L.A., and Bowie, A.G. (2007). The family of five: TIR-domain-containing adaptors in Toll-like receptor signalling. Nat. Rev. Immunol. *7*, 353–364.

Picard, C., von Bernuth, H., Ghandil, P., Chrabieh, M., Levy, O., Arkwright, P.D., McDonald, D., Geha, R.S., Takada, H., Krause, J.C., et al. (2010). Clinical features and outcome of patients with IRAK-4 and MyD88 deficiency. Medicine (Baltimore) *89*, 403–425.

Pichlmair, A., Lassnig, C., Eberle, C.A., Górna, M.W., Baumann, C.L., Burkard, T.R., Bürckstümmer, T., Stefanovic, A., Krieger, S., Bennett, K.L., et al. (2011). IFIT1 is an antiviral protein that recognizes 5′-triphosphate RNA. Nat. Immunol. *12*, 624–630.

Puente, X.S., Pinyol, M., Quesada, V., Conde, L., Ordóñez, G.R., Villamor, N., Escaramis, G., Jares, P., Beà, S., González-Díaz, M., et al. (2011). Whole-genome sequencing identifies recurrent mutations in chronic lymphocytic leukaemia. Nature *475*, 101–105.

Qureshi, N., Takayama, K., and Kurtz, R. (1991). Diphosphoryl lipid A obtained from the nontoxic lipopolysaccharide of Rhodopseudomonas sphaeroides is an endotoxin antagonist in mice. Infect. Immun. *59*, 441–444.

Rey, F.E., Cifuentes, M.E., Kiarash, A., Quinn, M.T., and Pagano, P.J. (2001). Novel competitive inhibitor of NAD(P)H oxidase assembly attenuates vascular O(2)(-) and systolic blood pressure in mice. Circ. Res. *89*, 408–414.

Savina, A., Jancic, C., Hugues, S., Guermonprez, P., Vargas, P., Moura, I.C., Lennon-Duménil, A.M., Seabra, M.C., Raposo, G., and Amigorena, S. (2006). NOX2 controls phagosomal pH to regulate antigen processing during crosspresentation by dendritic cells. Cell *126*, 205–218.

Schroder, K., and Tschopp, J. (2010). The inflammasomes. Cell *140*, 821–832.

Schroder, K., Zhou, R., and Tschopp, J. (2010). The NLRP3 inflammasome: a sensor for metabolic danger? Science *327*, 296–300.

Sinnett, D., Richer, C., Deragon, J.M., and Labuda, D. (1991). Alu RNA secondary structure consists of two independent 7 SL RNA-like folding units. J. Biol. Chem. *266*, 8675–8678.

Smith, W., Assink, J., Klein, R., Mitchell, P., Klaver, C.C., Klein, B.E., Hofman, A., Jensen, S., Wang, J.J., and de Jong, P.T. (2001). Risk factors for age-related macular degeneration: Pooled findings from three continents. Ophthalmology *108*, 697–704.

Streilein, J.W. (2003). Ocular immune privilege: therapeutic opportunities from an experiment of nature. Nat. Rev. Immunol. *3*, 879–889.

Sun, D., and Ding, A. (2006). MyD88-mediated stabilization of interferon-gamma-induced cytokine and chemokine mRNA. Nat. Immunol. *7*, 375–381.

Sun, Q., Sun, L., Liu, H.H., Chen, X., Seth, R.B., Forman, J., and Chen, Z.J. (2006). The specific and essential role of MAVS in antiviral innate immune responses. Immunity *24*, 633–642.

Suzuki, N., Suzuki, S., Duncan, G.S., Millar, D.G., Wada, T., Mirtsos, C., Takada, H., Wakeham, A., Itie, A., Li, S., et al. (2002). Severe impairment of interleukin-1 and Toll-like receptor signalling in mice lacking IRAK-4. Nature *416*, 750–756.

Suzuki, N., Chen, N.J., Millar, D.G., Suzuki, S., Horacek, T., Hara, H., Bouchard, D., Nakanishi, K., Penninger, J.M., Ohashi, P.S., and Yeh, W.C. (2003). IL-1 receptor-associated kinase 4 is essential for IL-18-mediated NK and Th1 cell responses. J. Immunol. *170*, 4031–4035.

Tabeta, K., Hoebe, K., Janssen, E.M., Du, X., Georgel, P., Crozat, K., Mudd, S., Mann, N., Sovath, S., Goode, J., et al. (2006). The Unc93b1 mutation 3d disrupts exogenous antigen presentation and signaling via Toll-like receptors 3, 7 and 9. Nat. Immunol. *7*, 156–164.

Takeda, A., Baffi, J.Z., Kleinman, M.E., Cho, W.G., Nozaki, M., Yamada, K., Kaneko, H., Albuquerque, R.J., Dridi, S., Saito, K., et al. (2009). CCR3 is a target for age-related macular degeneration diagnosis and therapy. Nature *460*, 225–230.

Thornberry, N.A., Bull, H.G., Calaycay, J.R., Chapman, K.T., Howard, A.D., Kostura, M.J., Miller, D.K., Molineaux, S.M., Weidner, J.R., Aunins, J., et al. (1992). A novel heterodimeric cysteine protease is required for interleukin-1 beta processing in monocytes. Nature *356*, 768–774.

Tschopp, J., and Schroder, K. (2010). NLRP3 inflammasome activation: The convergence of multiple signalling pathways on ROS production? Nat. Rev. Immunol. *10*, 210–215.

Tschopp, J., Martinon, F., and Burns, K. (2003). NALPs: a novel protein family involved in inflammation. Nat. Rev. Mol. Cell Biol. *4*, 95–104.

van Bruggen, R., Köker, M.Y., Jansen, M., van Houdt, M., Roos, D., Kuijpers, T.W., and van den Berg, T.K. (2010). Human NLRP3 inflammasome activation is Nox1-4 independent. Blood *115*, 5398–5400.

Vandenabeele, P., Vanden Berghe, T., and Festjens, N. (2006). Caspase inhibitors promote alternative cell death pathways. Sci. STKE *2006*, pe44.

Verhoef, P.A., Kertesy, S.B., Lundberg, K., Kahlenberg, J.M., and Dubyak, G.R. (2005). Inhibitory effects of chloride on the activation of caspase-1, IL-1beta secretion, and cytolysis by the P2X7 receptor. J. Immunol. *175*, 7623–7634.

Vogt, S.D., Curcio, C.A., Wang, L., Li, C.M., McGwin, G., Jr., Medeiros, N.E., Philp, N.J., Kimble, J.A., and Read, R.W. (2011). Retinal pigment epithelial expression of complement regulator CD46 is altered early in the course of geographic atrophy. Exp. Eye Res. *93*, 413–423.

von Bernuth, H., Picard, C., Jin, Z., Pankla, R., Xiao, H., Ku, C.L., Chrabieh, M., Mustapha, I.B., Ghandil, P., Camcioglu, Y., et al. (2008). Pyogenic bacterial infections in humans with MyD88 deficiency. Science *321*, 691–696.

Wen, H., Gris, D., Lei, Y., Jha, S., Zhang, L., Huang, M.T., Brickey, W.J., and Ting, J.P. (2011). Fatty acid-induced NLRP3-ASC inflammasome activation interferes with insulin signaling. Nat. Immunol. *12*, 408–415.

Yamamoto, M., Sato, S., Hemmi, H., Hoshino, K., Kaisho, T., Sanjo, H., Takeuchi, O., Sugiyama, M., Okabe, M., Takeda, K., and Akira, S. (2003). Role of adaptor TRIF in the MyD88-independent toll-like receptor signaling pathway. Science *301*, 640–643.

Yang, Y.L., Reis, L.F., Pavlovic, J., Aguzzi, A., Schäfer, R., Kumar, A., Williams, B.R., Aguet, M., and Weissmann, C. (1995). Deficient signaling in mice devoid of double-stranded RNA-dependent protein kinase. EMBO J. *14*, 6095–6106.

Zaki, M.H., Boyd, K.L., Vogel, P., Kastan, M.B., Lamkanfi, M., and Kanneganti, T.D. (2010). The NLRP3 inflammasome protects against loss of epithelial integrity and mortality during experimental colitis. Immunity *32*, 379–391.

Zhou, R., Yazdi, A.S., Menu, P., and Tschopp, J. (2011). A role for mitochondria in NLRP3 inflammasome activation. Nature *469*, 221–225.